Phys. Status Solidi A **210**, No. 5, 898–904 (2013) / **DOI** 10.1002/pssa.201200930

physica status solidi pss a
www.pss-a.com
applications and materials science

Part of Special Section on Engineering of Functional Interfaces

Multi-sensor chip for the investigation of different types of metal oxides for the detection of H_2O_2 in the ppm range

Steffen Reisert[1], Benno Schneider[1], Hanno Geissler[2], Matthias van Gompel[3], Patrick Wagner[3], and Michael J. Schöning[*,1,4]

[1] Institute of Nano and Biotechnologies, FH Aachen, Heinrich-Mußmann-Straße 1, 52428 Jülich, Germany
[2] SIG Combibloc Systems GmbH, Rurstraße 58, 52441 Linnich, Germany
[3] Institute for Materials Research, Hasselt University, Wetenschapspark 1, 3590 Diepenbeek, Belgium
[4] Peter Grünberg Institute, Research Centre Jülich GmbH, 52425 Jülich, Germany

Received 7 November 2012, revised 10 January 2013, accepted 4 February 2013
Published online 4 March 2013

Keywords doped metal oxide, gas sensor, hydrogen peroxide, multi-sensor, tin oxide, tungsten oxide

* Corresponding author: e-mail schoening@fh-aachen.de, Phone: +49 241 6009 53215, Fax: +49 241 6009 53235

In this work, a multi-sensor chip for the investigation of the sensing properties of different types of metal oxides towards hydrogen peroxide in the ppm range is presented. The fabrication process and physical characterization of the multi-sensor chip are described. Pure SnO_2 and WO_3 as well as Pd- and Pt-doped SnO_2 films are characterized in terms of their sensitivity to H_2O_2. The sensing films have been prepared by drop-coating of water-dispensed nano-powders. A physical characterization, including scanning electron microscopy and X-ray diffraction analysis of the deposited metal-oxide films, was done. From the measurements in hydrogen peroxide atmosphere, it could be shown, that all of the tested metal oxide films are suitable for the detection of H_2O_2 in the ppm range. The highest sensitivity and reproducibility was achieved using Pt-doped SnO_2.

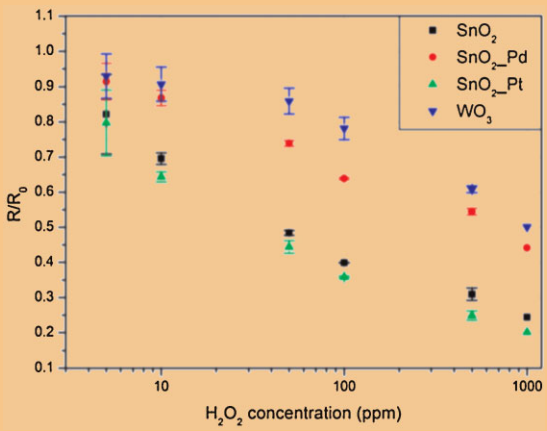

Calibration plot of a SnO_2, WO_3, Pt-, and Pd-doped SnO_2 gas sensor for H_2O_2 concentrations in the ppm range.

1 Introduction Hydrogen peroxide (H_2O_2) is a commonly used sterilizing agent for carton packages in aseptic food filling processes. Due to its ability to decompose to water and oxygen it is advantageous compared to other chemical sterilization agents in terms of environmental compatibility [1]. However, in view of its strong oxidizing properties, special precautions with regard to the workplace security in the surrounding of sterilization plants employing H_2O_2 as sterilizing agent have to be taken into account, especially when applied in vapor phase. Therefore, the American Conference of Governmental Industrial Hygienists (ACGIH) has assigned hydrogen peroxide a threshold limit value (TLV) of 1 ppm. For monitoring the concentration in danger zones and in the workplace environment, electrochemical sensor systems from the German company *Dräger* have been established. These monitoring systems typically cover a measuring range either in the lower (0–20 ppm) or in the upper (1000–7000 ppm) range, but nothing in between or beyond that, nor are these operable in high flow conditions. With regard to the aseptic filling processes, there is a high demand for monitoring the H_2O_2 concentration in the exhaust air of such sterilization plants, which typically is in the ppm concentration range, not only with respect to the TLV but also in terms of process monitoring.

Previous works have shown that calorimetric-type gas sensors are suitable for monitoring H_2O_2 concentrations in the range between 1 and 8% v/v [2–6]. This is equally true for commercially available metal-oxide-semiconductor gas sensors [7]. While the lower limit of detection (LOD) in case of the calorimetric gas sensors, which determine the exothermic energy due to a catalytic reaction, is in the range of approximately 5000 ppm, it is assumed that metal-oxide gas sensors respond at lower concentrations. Within the frame of this work, different types of metal oxides shall be investigated on their response to H_2O_2 in the range between 5 and 1000 ppm. Therefore, a multi-sensor chip, including four individually controllable sensor structures, based on a sapphire substrate with the size of $8 \times 8\,mm^2$ has been developed. The four sensor structures have been prepared with different types of metal oxides. On one hand, two of the structures were prepared with pure tin oxide (SnO_2) and tungsten oxide (WO_3) films. On the other hand, two sensor structures have been prepared with palladium- (Pd) and platinum black- (Pt) doped SnO_2, respectively. The doping of metal oxides with catalytically active species is a common strategy to enhance catalytical effects at the sensor surface, in order to increase the sensitivity and selectivity of semiconductor gas sensors for certain gas molecules [8–11]. Typical amounts of such a dopant are in the range between 0.1 and 2% w/w [12, 13].

2 Experimental

2.1 Sensor fabrication The multi-sensor chip fabricated in this work contains four identical sensing structures on a sapphire substrate with a size of $8 \times 8\,mm^2$. Sapphire was used as substrate due to its thermal properties. It has a lower thermal conductivity (sapphire: $35\,W\,mK^{-1}$ @ 300 K) compared to common substrate materials, like silicon (Si: $148\,W\,mK^{-1}$ @ 300 K), for instance. A low thermal conductivity is beneficial for a thermal insulation between the individual sensing structures on the multi-sensor chip. Furthermore, it offers high chemical stability and good thermal shock properties. Each one of the sensing structure consists of an interdigitated electrode (IDE) and a heating element. The size of the heater is approximately $0.9 \times 0.9\,mm^2$. A schematic of the sensor chip is shown in Fig. 1.

The sensor chips were fabricated on a 3'' sapphire wafer with a thickness of $430 \pm 20\,\mu m$. The IDE and heating elements, which consist of 200 nm platinum (Pt) and a 20 nm titanium (Ti) adhesion layer, were deposited by thermal evaporation and patterned by a lift-off process. Subsequently, a 500 nm alumina (Al_2O_3) layer was deposited by E-beam evaporation as passivation. As a last step, the Al_2O_3 layer was patterned by chemical wet etching (Micropur, BOE 7:1, 9 min) [14] in order to uncover the contact pads and IDE.

2.2 Sensor preparation On each one of the four structures on the chip a sensitive metal-oxide film has been deposited. As sensitive materials, n-type tin(IV)-oxide (SnO_2) and tungsten(IV)-oxide (WO_3), respectively, were used. While two of the structures were prepared with pure SnO_2 and WO_3, the remaining two structures have been prepared with palladium- (Pd) and platinum black- (Pt) doped SnO_2, respectively. The metal oxides were available as nano-powder with a particle size smaller than 100 nm (Sigma–Aldrich, Germany). One-hundred and forty milligrams of the powders were dispersed in 1 ml distilled water [15], while the dispersions for the preparation of the Pd- and Pt-doped films contained 0.5% w/w of platinum black (<20 μm, Sigma–Aldrich, Germany) and palladium (<1 μm, Sigma–Aldrich, Germany) powder, respectively [16]. The composition of the different dispersions is summarized in Table 1.

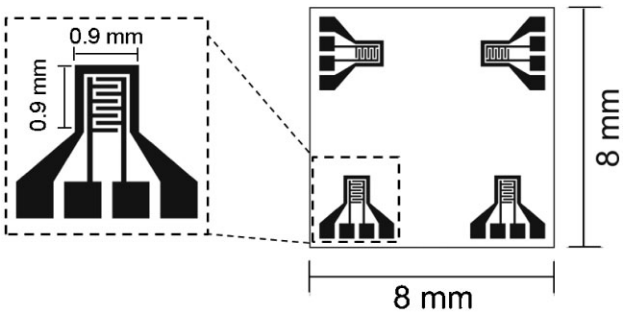

Figure 1 Schematic of the multi-sensor chip on a sapphire substrate, containing four sensing structures with embedded heater (outer structure) and IDEs (inner structure).

The dispersions were drop-coated onto the sensor surface with a drop volume of 0.5 μl. Afterwards, the chip was heated up to approximately 320 °C in order to evaporate the water and to provide adhesion of the sensing layer. A calcination of the metal-oxide films at higher temperatures than 320 °C had to be avoided due to the fact that the thin-film resistances suffered changes in their electrical properties, as will be discussed in more detail in Section 2.3.3. Nevertheless, it was shown in previous studies, that the catalytic activity of the dopants towards H_2O_2 is already activated at temperatures below 300 °C [4]. Figure 2a provides an image of the sensor chip after the deposition of the semiconductor films. The order of the sensing films as they were deposited onto the substrate is shown in Fig. 2b.

2.3 Characterization

2.3.1 XRD Prior to the preparation of the sensor chip, the metal-oxide powders, namely SnO_2 and WO_3, were

Table 1 Composition of the dispersions used for the preparation of the sensing films.

spot	metal oxide	dopant	dispensed in
1	SnO_2 (140 mg)	none	dest. water (1 ml)
2	SnO_2 (140 mg)	Pt (0.5% w/w)	dest. water (1 ml)
3	SnO_2 (140 mg)	Pd (0.5% w/w)	dest. water (1 ml)
4	WO_3 (140 mg)	none	dest. water (1 ml)

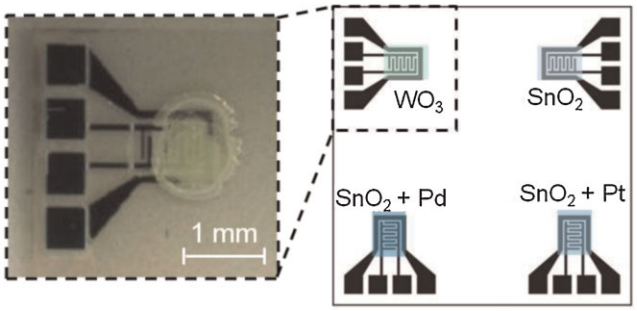

Figure 2 (online color at: www.pss-a.com) Microscopic image of the multi-sensor chip after the deposition of the sensing layers and schematic of the distribution of the sensing films on the chip.

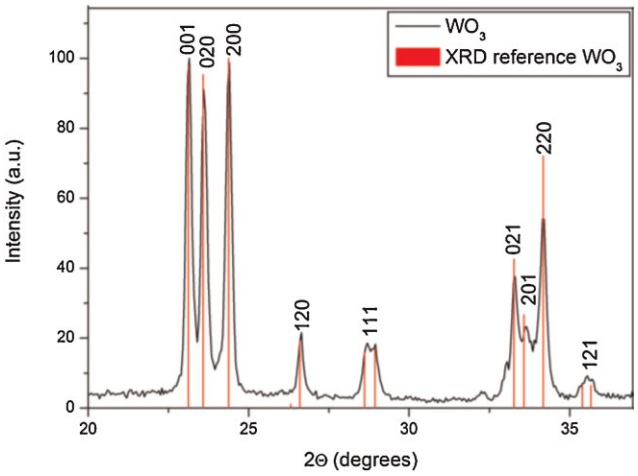

Figure 4 (online color at: www.pss-a.com) Indexed XRD spectrum of WO_3 nano-powder prepared on a silicon substrate recorded in a two-theta angle range from 20° to 37°.

investigated by X-ray diffraction analysis (XRD). Contrary to the final sensor chips, the test samples of the pure metal oxides have been prepared onto a silicon substrate as the sapphire substrates have not been available at the time of material characterization. To ensure that the results of the test samples are transferrable to the sapphire substrate, the sensitive films have been prepared in an analogous manner (see section 2.2). A Siemens D5000 diffractometer with Cu Kα radiation ($\lambda = 1.540598$ Å) was used to record the spectra. The XRD spectra of SnO_2 (Fig. 3) and WO_3 (Fig. 4) were monitored in a two-theta angle range from 20° to 65° and 20° to 37°, respectively.

The diffraction peaks in the XRD pattern can be indexed to the rutile phase SnO_2 and orthorhombic crystal structure in case of WO_3, respectively, as provided by Urusov et al. [17] and Loopstra and Boldrini [18]. No characteristic peaks of impurities, such as pure metals or surfactants, were observed. The average size of the crystallites were deduced from Scherrer's formula for the strongest peaks and found to be 14 nm in case of SnO_2 and 27 nm in case of WO_3.

2.3.2 SEM In order to investigate the morphology of the sensing films, the same type of samples as used for XRD have been analyzed by scanning electron microscopy (SEM), as the sapphire substrates had not been available at the time of material characterization. Still, the properties of the sensing films should be comparable to those on sapphire substrate as the method of preparation was exactly the same. Figures 5 and 6 show the SEM images of the prepared samples with SnO_2 (Fig. 5) and WO_3 (Fig. 6) with a magnification of approximately 100 k.

Both, the SnO_2 and WO_3 samples depict a rough and highly covered surface, which is favorable in terms of gas sensing, especially in the lower concentration range. The average size of the crystallites observed in SEM images is consistent with the results obtained from the XRD patterns.

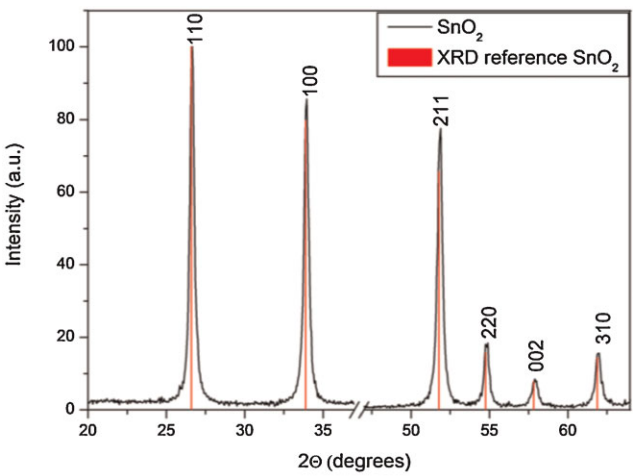

Figure 3 (online color at: www.pss-a.com) Indexed XRD spectrum of SnO_2 nano-powder prepared on a silicon substrate recorded in a two-theta angle range from 20° to 65°.

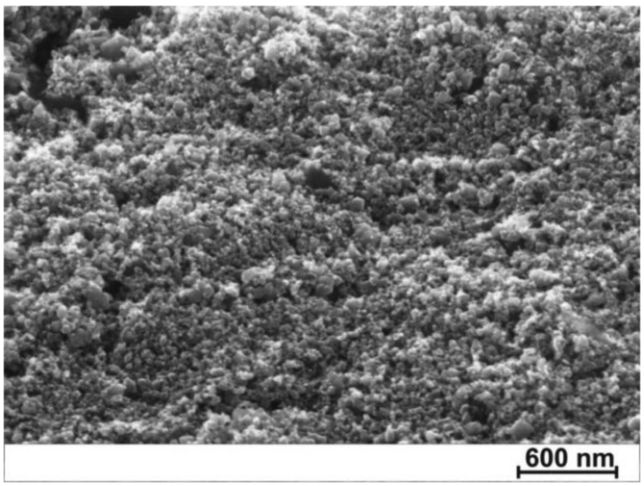

Figure 5 SEM image of an SnO_2 film prepared on a silicon substrate at a magnification of approximately 100 k.

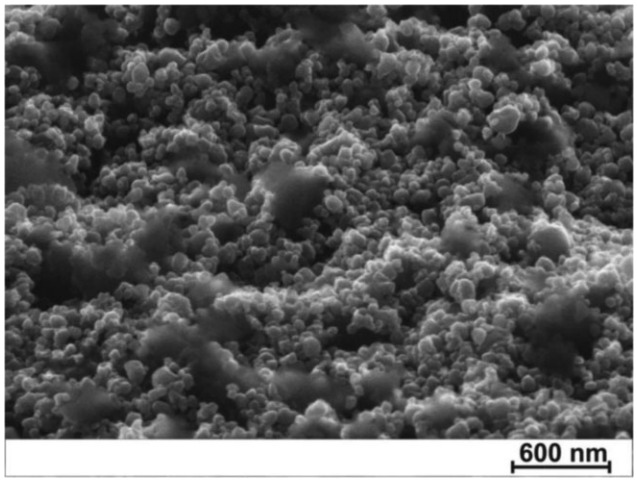

Figure 6 SEM image of a WO_3 film prepared on a silicon substrate at a magnification of approximately 100 k.

2.3.3 Thermal characterization In order to determine the resistance (R_0) and thermal coefficient (α) of the heating elements, a comparison calibration in a defined temperature bath has been done in several steps between 20 and 80 °C. From the average of four sensor chips (16 heaters) out of one charge, R_0 was found to be $17.41 \pm 0.64\,\Omega$ and $\alpha = 3.12 \times 10^{-3} \pm 3.4 \times 10^{-5}\,K^{-1}$. The determined value for α is in good accordance with the values obtained for Ti/Pt thin-film resistances by Groenland [19].

The sensor chip was designed in a way that each sensing structure can be heated individually. Nevertheless, for the sensor characterization the four heaters were operated with a single voltage source in parallel. In order to achieve an operating temperature of 320 ± 2 °C in the gas stream (air flow of $70\,m^3\,h^{-1}$, gas temperature of 70 °C), a voltage of 6 V was applied to the heaters, resulting in a current of 688 mA and an overall power consumption of 4.1 W.

In a further experiment, it was found that an excessive heating of the sensor chips caused changes in the electric properties of the heating elements. At chip temperatures >400 °C, the platinum–titanium bilayer thin-film resistances were subject to interlayer diffusion and stress-induced morphological changes, as it was confirmed by the investigations of Groenland [19]. This leaded to an >100% increase of the nominal resistance R_0 as well as to changes in the thermal coefficient α. In order to avoid changes in the thermal properties of the sensor chip during the film deposition and later on during the measurements, its maximum operating temperature had to be reduced to 320 °C.

2.4 Experimental set-up For the characterization of the sensing properties, the sensor chip was attached to a printed circuit board (PCB) and contacted via bond wires. The sensor chip was located in the exhaust pipe of an aseptic sterilization chamber, which is continuously flooded with hydrogen peroxide vapor. Therefore, a technical grade aqueous hydrogen peroxide solution of 35% w/w is fed to a flow-controlled air stream, which is supplied by compressed air. Subsequently, the gas–liquid-mixture is evaporated in a heater. For a detailed description of the H_2O_2-vapor generation unit is referred to Ref. [4]. While hydrogen peroxide is vaporized into the chamber at an air flow of $10\,m^3\,h^{-1}$, the exhauster provides a continuously discharge of $70\,m^3\,h^{-1}$. The $60\,m^3\,h^{-1}$ lack between the H_2O_2 vapor entry ($10\,m^3\,h^{-1}$) and the suction capacity of the exhauster ($70\,m^3\,h^{-1}$) is being compensated by aspiration of ambient air via venting slots. As a result, the H_2O_2 concentration in the exhausted air is being diluted to 1/7 of its initial concentration in gaseous phase. Since, according to the knowledge of the authors, no reference method for the detection of hydrogen peroxide under the given conditions (broad concentration range and high flow) has been available, it was assumed that the dosed amount of hydrogen peroxide fully passes over into the gaseous phase and will be present at the point of measurement. The discharge of $70\,m^3\,h^{-1}$ was checked with a flow meter. The diameter of the exhaust pipe is 10 cm. A schematic of the experimental set-up is shown in Fig. 7.

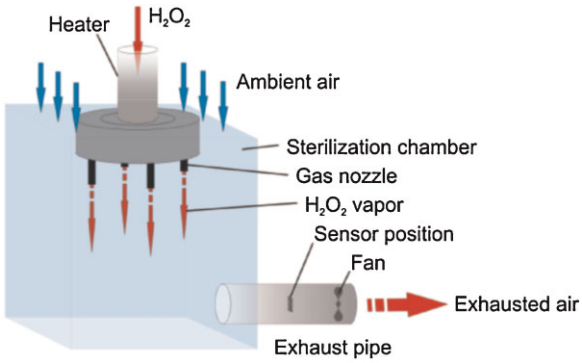

Figure 7 (online color at: www.pss-a.com) Schematic of the experimental set-up for the generation of hydrogen-peroxide vapor.

3 Results and discussion

3.1 Measurements For the characterization of the sensor response to hydrogen peroxide, various concentrations of H_2O_2 in the exhaust air stream, ranging from 5 to 1000 ppm, have been provided. The concentration steps in between were 10, 50, 100, and 500 ppm, respectively. After the vaporization system was heated up to a stable operating temperature, the vaporization by H_2O_2 was started. Initially, a concentration of 5 ppm H_2O_2 was provided for 10 min, following a stepwise increase of the H_2O_2 concentration up to the maximum concentration of 1000 ppm and in return a stepwise decrease down to 5 ppm. Each concentration step was kept for 10 min. The hydrogen peroxide has been vaporized to the sterilization chamber at a temperature of 270 °C. By dilution with ambient air, the gas stream reaches a temperature of about 70 °C in the exhaust pipe.

3.2 H_2O_2 sensing The sensor chip with four different types of metal-oxide films was investigated for H_2O_2 concentrations between 5 and 1000 ppm. Figure 8 presents the recorded measurement data for the SnO_2 as well as Pd- and Pt-doped SnO_2 films in one diagram.

Prior to the exposure of H_2O_2, the system has to reach steady conditions in terms of flow and temperature in the exhaust pipe ($t < 70$ min). In this way, it was also ensured that the operating temperature of the sensor chip is not being influenced by alterations of the temperature in the exhaust air. This condition was assumed to be fulfilled when the relative change in resistance of the sensing films was less than 1% of the absolute resistance value per minute ($t = 70$ min). At this point, the resistances are in the same order of magnitude between approximately 60 and 90 MΩ. To the exposure of H_2O_2, the sensors respond with a decrease in their resistance and with further increase of the H_2O_2 concentration, the resistances of the different sensors decrease gradually. After the exposure to the highest concentration of 1000 ppm H_2O_2, the resistance values raise again towards lower concentrations. After the exposure to H_2O_2 was stopped at $t = 182$ min, the resistances of the SnO_2 and Pt-doped SnO_2 films raise to similar values as prior to the exposure of H_2O_2 ($t = 70$ min). In case of the Pd-doped sensor, the resistance of the sensing film is somewhat lower compared to its initial value.

The resistance behavior of the WO_3 sensor was recorded in parallel and is shown in Fig. 9.

The initial resistance value of the WO_3 film is around 20 MΩ, thus slightly lower compared to the SnO_2 and doped SnO_2 films. The response of the WO_3 sensor is similar compared to the other sensors, however, it is subject to a higher drift.

In order to characterize the sensor behavior and to compare the different materials, the relative resistance values of all sensors were plotted in a single diagram. Therefore, the resistance values (R) of the individual sensors at each concentration step were divided by the initial resistance value (R_0) before the exposure to H_2O_2 ($t = 70$ min). Figure 10 overviews the calibration plots of the four sensors for a logarithmic scale of the H_2O_2 concentration. The plotted values correspond to the mean values of the sensor signals for equal concentrations, recorded once towards higher concentrations and towards lower concentrations, respectively. The error bars represent the standard deviation of these values.

All types of sensors exhibit a linear correlation between the change in their relative resistance and the logarithm of the H_2O_2 concentration in the range between 5 and 1000 ppm. The lowest sensitivity was observed for the WO_3 film, followed by the Pd-doped SnO_2 sensor. Also, the reproducibility of the WO_3 sensor is lower compared to the other ones (compare error bars in Fig. 10). The Pt-doped SnO_2 offered the highest sensitivity to H_2O_2 in the ppm range, whereas it was slightly lower in case of undoped SnO_2. The LOD for hydrogen peroxide was found to be 5 ppm in

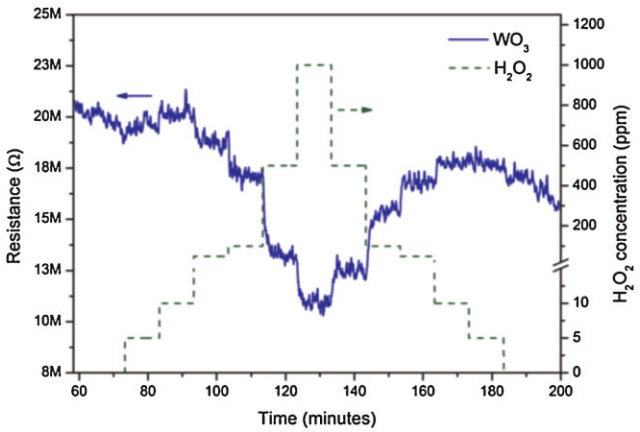

Figure 9 (online color at: www.pss-a.com) Measurement data of the WO_3 gas sensor in hydrogen peroxide atmosphere.

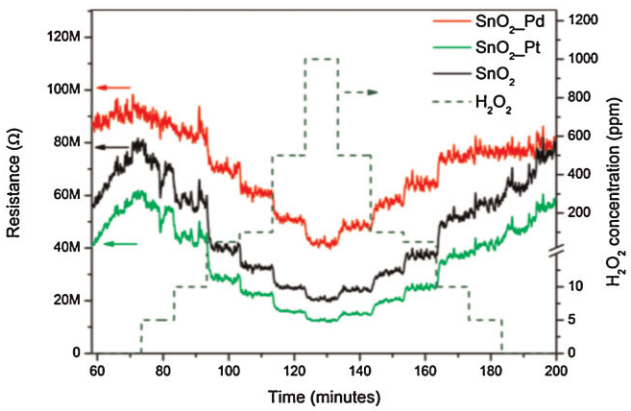

Figure 8 (online color at: www.pss-a.com) Measurement data of the undoped, Pt-, and Pd-doped SnO_2 gas sensors in hydrogen peroxide atmosphere.

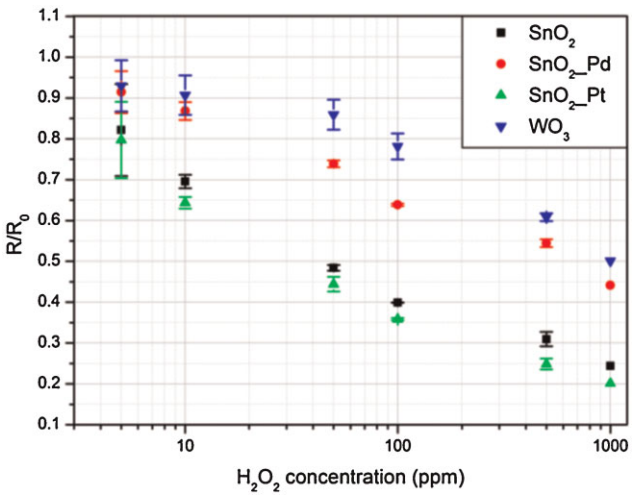

Figure 10 (online color at: www.pss-a.com) Calibration plot of a SnO_2, WO_3, Pt-, and Pd-doped SnO_2 gas sensor for H_2O_2 concentrations in the ppm range.

case of the undoped and Pt-doped SnO_2, 10 ppm for Pd-doped SnO_2 and 50 ppm in case of the WO_3 film.

Considering the relative resistance changes of the sensitive layers, it is found that, for example, in case of the undoped SnO_2 sensor, the relative change of the resistance (R/R_0) upon exposure of hydrogen peroxide is about 1/2.5 per decade. This seems somewhat low compared to the sensitivities that are typically achieved with n-type semiconductor gas sensors when exposed to oxidizing or reducing gases. These are typically in the range of 3/1 for oxidizing gases such as O_2 up to a ratio of 5/1 for reducing gases such as H_2 or methane, for instance [20]. In earlier works however, similar sensitivities as by the results presented here have been observed upon the exposure of commercially available n-type semiconductor gas sensors with H_2O_2 in the lower percent range [7].

The fact that the resistivity of the sensors decreases under exposure to H_2O_2 seems not to be in accordance with the expected behavior of n-type metal-oxide-semiconductor materials, which exclusively were used in this case, when in contact to oxidizing gases, like hydrogen peroxide. It is generally considered that, in case of n-type metal-oxide-semiconductor gas sensors, reducing gases react with adsorbed oxygen ions at the metal-oxide surface, so releasing bound electrons, which are then free to conduct. As a result, the resistance of the surface layer decreases. For an oxidizing gas, the converse mechanism will operate and the resistance will rise [21]. Though, the same type of behavior was observed in previous studies for the exposure to H_2O_2 in a higher concentration range using commercially available n-type semiconductor gas sensors with not exactly specified composition of the sensing films [7]. To explain the decrease of the resistance with increasing H_2O_2 concentration, one has additionally to take into consideration the mechanism of reaction concerning the decomposition of H_2O_2. Although the complete mechanism is not completely uncovered yet, H_2O_2 is known to decompose to H_2O and O_2 following a pathway provided by Hiroki and LaVerne [22]:

$$H_2O_2 \rightarrow 2OH^{\bullet}, \quad (1)$$

$$OH^{\bullet} + H_2O_2 \rightarrow HO_2 + H_2O, \quad (2)$$

$$2HO_2 \rightarrow H_2O_2 + O_2. \quad (3)$$

The occurrence of hydroxyl radicals ($OH^{\cdot}$) according to Eq. (2), knowing they are of transitory nature, was proven to have a strong influence on the electrical conductivity of n-type metal oxides as they react with adsorbed oxygen molecules at the metal-oxide surface leading to a decrease in the resistance [23]. As Pd and Pt are known to have a high catalytic activity towards H_2O_2 [15] it was presumed that doping by these two materials may increase the sensitivity due to an enhanced reaction of H_2O_2 at the metal-oxide surface. In case of the Pt-doped SnO_2 a slightly higher sensitivity compared to the undoped SnO_2 was observed, which might be the result of a catalytical reaction of H_2O_2 at the Pt particles. In case of the Pd-doped SnO_2, which exhibits a lower sensitivity to H_2O_2 compared to undoped SnO_2, the sensing mechanism seems to be more complex. One proposal could be that the Pd particles catalytically activate the dissociation of molecular oxygen. As a result, its atomic products then diffuse to the metal oxide increasing both, the quantity of oxygen that will rebind vacancies on the SnO_2 surface as well as the rate at which rebinding occurs, resulting in a greater degree of electron withdrawal from the SnO_2. This mechanism is well established in the catalysis literature and dates back to the 1960s. In this context, Boudart et al. [24] coined the term "spillover effect".

The impact of humidity on the sensor response has not been studied in detail. Generally, n-type semiconductors as the presented SnO_2 and WO_3 gas sensors are known to be humidity-sensitive. As for the sensor calibration a 35% w/w aqueous hydrogen peroxide solution was used, the H_2O_2 concentrations in gaseous phase have been regulated by adjusting the dosed amount of the aqueous solution. It is therefore generally assumed that H_2O_2 and H_2O will be present in the same mass ratio, regardless of the absolute dosage. In this way, similar conditions arise upon the exposure to different concentrations of hydrogen peroxide. Measurements with commercially available sensors of the same type under H_2O_2 atmosphere have shown that H_2O shifted the sensor signal of an n-type semiconductor in the same direction such as hydrogen peroxide. However, the response on H_2O_2 was about ten times higher [7].

4 Conclusions A multi-sensor chip with four individually controllable sensing structures was fabricated and deposited with different types of metal oxides. Both, the SnO_2 and WO_3 layers seem to be promising candidates for hydrogen peroxide sensing in the ppm concentration range. Regarding the sensing mechanism of the doped SnO_2 films, still some questions remain unanswered. However, it could be shown that doping of SnO_2 by platinum black increases the sensitivity towards H_2O_2.The lower detection limit was found to be 5 ppm. In this study, SnO_2 films showed a higher reproducibility compared to WO_3 films.

Even though that the sensor response on H_2O_2 is less pronounced as compared to typical target gases such as hydrocarbons, its usability in the illustrated application seems justified, as there are currently no suitable reference methods for the detection of hydrogen peroxide in exhaust systems that cover such wide measuring range, which potentially spans from the low ppm range up to the percent range. A statement on the lifetime of the multi-sensor, especially in continuous use under exposure to H_2O_2, cannot be taken at this time. However, a lifetime of several months would be desirable and seems to be reasonable. Another challenge is yet to detect H_2O_2 concentrations below 5 ppm, to make the sensor feasible for workplace monitoring in terms of TLV.

Acknowledgements The authors thank Hans-Peter Bochem from the Research Centre Jülich for the SEM images.

References

[1] S. Reisert, H. Henkel, A. Schneider, D. Schäfer, P. Friedrich, J. Berger, and M. J. Schöning, Phys. Status Solidi A **207**, 913 (2010).
[2] N. Näther, H. Henkel, A. Schneider, and M. J. Schöning, Phys. Status Solidi A **206**, 449 (2009).
[3] N. Näther, R. Emmerich, J. Berger, P. Friedrich, H. Henkel, A. Schneider, and M. J. Schöning, Sensors **6**, 308 (2006).
[4] P. Kirchner, B. Li, H. Spelthahn, H. Henkel, A. Schneider, P. Friedrich, J. Kolstad, M. Keusgen, and M. J. Schöning, Sens. Actuators B **154**, 257 (2011).
[5] P. Kirchner, Y. A. Ng, H. Spelthahn, A. Schneider, H. Henkel, P. Friedrich, J. Kolstad, J. Berger, M. Keusgen, and M. J. Schöning, Phys. Status Solidi A **207**, 787 (2010).
[6] P. Kirchner, J. Oberländer, P. Friedrich, J. Berger, H. P. Suso, A. Kupyna, M. Keusgen, and M. J. Schöning, Phys. Status Solidi A **208**, 1235 (2011).
[7] S. Reisert, H. Geissler, R. Flörke, N. Näther, P. Wagner, and M. J. Schöning, Phys. Status Solidi A **208**, 1351 (2011).
[8] P. Ménini, F. Parret, M. Guerrero, K. Soulantica, L. Erades, A. Maisonnat, and B. Chaudret, Sens. Actuators B **103**, 111 (2004).
[9] L. K. Bagal, J. Y. Patil, I. S. Mulla, and S. S. Suryavanshi, Ceram. Int. **38**, 4835 (2012).
[10] G. Korotcenkov, V. Brinzari, Y. Boris, M. Ivanov, J. Schwank, and J. Morante, Thin Solid Films **436**, 119 (2003).
[11] Y. C. Lee, H. Huang, O. K. Tan, and M. S. Tse, Sens. Actuators B **132**, 239 (2008).
[12] V. N. Mishra, and R. P. Agarwal, Microelectron. J. **29**, 861 (1998).
[13] J. K. Srivastava, P. Pandey, V. N. Mishra, and R. Dwivedi, Solid State Sci. **11**, 1602 (2009).
[14] K. Williams, K. Gupta, and M. Wasilik, J. Microelectromech. Syst. **12**, 761 (2003).
[15] J.-H. Smått, M. Lindén, T. Wagner, C.-D. Kohl, and M. Tiemann, Sens. Actuators B **155**, 483 (2011).
[16] N. Yamazoe, G. Sakai, and K. Shimanoe, Catal. Surv. Asia **7**, 63 (2003).
[17] V. Urusov, O. Yakubovich, and N. Eremin, Dokl. RAN **336**, 330 (1994).
[18] B. Loopstra, and P. Boldrini, Acta Cryst. **21**, 158 (1966).
[19] A.-W. Groenland, Degradation processes of platinum thin films on a silicon nitride surface, Research report, Transducers Science and Technology Group (2004).
[20] P. K. Clifford, and D. T. Tuma, Sens. Actuators **3**, 233 (1982).
[21] J. Watson, Sens. Actuators **5**, 29 (1984).
[22] A. Hiroki, and J. A. LaVerne, J. Phys. Chem. B **109**, 3364 (2005).
[23] C. M. Lousada, A. J. Johansson, T. Brinck, and M. Jonsson, J. Phys. Chem. C **116**, 9533 (2012).
[24] M. Boudart, M. A. Vannice, and J. E. Z. Benson, Phys. Chem. **64**, 171 (1969).

